Low Mechanical Loss TiO$_2$:GeO$_2$ Coatings for Reduced Thermal Noise in Gravitational Wave Interferometers

Gabriele Vajente[1,*] Le Yang[2] Aaron Davenport,[3] Mariana Fazio,[3] Alena Ananyeva,[1] Liyuan Zhang,[1]
Garilynn Billingsley,[1] Kiran Prasai,[4] Ashot Markosyan,[4] Riccardo Bassiri[4] Martin M. Fejer,[4]
Martin Chicoine,[5] François Schiettekatte[5] and Carmen S. Menoni[2,3]

[1]*LIGO Laboratory, California Institute of Technology, Pasadena, California 91125, USA*
[2]*Department of Chemistry, Colorado State University, Fort Collins, Colorado 80523, USA*
[3]*Department of Electrical and Computer Engineering, Colorado State University, Fort Collins, Colorado 80523, USA*
[4]*Edward L. Ginzton Laboratory, Stanford University, Stanford, California 94305, USA*
[5]*Département de Physique, Université de Montréal, Montréal, Québec H3T 1J4, Canada*

The sensitivity of current and planned gravitational wave interferometric detectors is limited, in the most critical frequency region around 100 Hz, by a combination of quantum noise and thermal noise. The latter is dominated by Brownian noise: thermal motion originating from the elastic energy dissipation in the dielectric coatings used in the interferometer mirrors. The energy dissipation is a material property characterized by the mechanical loss angle. We have identified mixtures of titanium dioxide (TiO$_2$) and germanium dioxide (GeO$_2$) that show internal dissipations at a level of 1×10^{-4}, low enough to provide improvement of almost a factor of 2 on the level of Brownian noise with respect to the state-of-the-art materials. We show that by using a mixture of 44% TiO$_2$ and 56% GeO$_2$ in the high refractive index layers of the interferometer mirrors, it would be possible to achieve a thermal noise level in line with the design requirements. These results are a crucial step forward to produce the mirrors needed to meet the thermal noise requirements for the planned upgrades of the Advanced LIGO (Laser Interferometer Gravitational-Wave Observatory) and Virgo detectors.

Gravitational wave (GW) detectors are highly sensitive instruments that measure the very small distance changes produced by signals of astrophysical origin [1,2]. The current generation of GW detectors are km-scale laser interferometers [3–6] with several hundreds of kW of circulating power in the Fabry-Perot arm cavities. The test-mass mirrors are made of high-purity fused silica substrates, coated with high-reflectivity multilayer dielectric thin-film stacks [7], composed of multiple pairs of high and low refractive index metal oxide layers, making a Bragg reflector structure.

The sensitivity of the current detectors [8,9] is limited by a combination of laser quantum noise [10] and displacement noise generated by the Brownian motion of the coatings [11,12]. Therefore, to increase the astrophysical reach of future detectors, it is crucial to reduce coating Brownian noise. This in turn requires reducing the elastic energy dissipation in the thin-film materials composing the coatings [12,13]. The power spectral density of Brownian noise at a frequency f is a complex function of the properties of the materials used in the coatings [14,15]. An approximate expression, assuming equal bulk and shear loss angles, is given by (see [15] and Supplemental Material [16]):

$$S_B(f) = \frac{2k_B T d}{\pi^2 w^2 f} \left[\left\langle \frac{Y}{1-\nu^2}\phi \right\rangle \frac{(1+\nu_S)^2(1-2\nu_S)^2}{Y_S^2} + \left\langle \frac{(1+\nu)(1-2\nu)}{(1-\nu)Y}\phi \right\rangle \right] \quad (1)$$

where k_B is the Boltzmann's constant, T is the ambient temperature, w is the radius of the laser beam probing the mirror motion, d is the total thickness of the coating, and Y_S and ν_S are the Young's modulus and Poisson ratio of the substrate. The angular bracket expression $\langle x \rangle$ indicates the *effective medium* average [15,21] of the material property x through the stack, weighted by the physical thickness of the layers. The relevant properties of the coating materials are the Young's moduli Y, the Poisson ratios ν, and the loss angles $\phi = \mathrm{Im}(Y)/\mathrm{Re}(Y)$.

The coatings used in the current Advanced Laser Interferometer Gravitational-Wave Observatory (LIGO) mirrors are composed of alternating layers of amorphous SiO$_2$ of low refractive index $n_{\mathrm{SiO_2}} = 1.45$ at 1064 nm, and TiO$_2$:Ta$_2$O$_5$ of high refractive index $n_{\mathrm{TiO_2:Ta_2O_5}} = 2.10$ at 1064 nm [22,23]. The TiO$_2$:Ta$_2$O$_5$ layers have a loss angle much larger than the SiO$_2$ layers (3–4×10^{-4} [24,25]

compared with $\sim 2 \times 10^{-5}$ [22]) and therefore they dominate in the contribution to the coating Brownian noise.

The goal for the next upgrade to the LIGO detectors, called Advanced LIGO+ [26,27] is a reduction of the coating noise by about a factor of 2, with a target Brownian noise of $S_B^{1/2} = 6.6 \times 10^{-21}$ m/$\sqrt{\text{Hz}}$ at a frequency of 100 Hz. The SiO$_2$ layers can already be produced with low enough mechanical loss angle [22], so the main focus of the current research is on improving the high refractive index material. Several different approaches have been investigated, including deposition at elevated substrate temperatures [28,29] and with assist ion bombardment [30,31], doping and nanolayering of Ta$_2$O$_5$ [32–35], and the use of nitrides [36,37]. Here we report results on amorphous oxide coatings based on mixtures of GeO$_2$ and TiO$_2$.

The initial motivation to investigate coatings based on GeO$_2$ was the discovery of a correlation between the room-temperature mechanical loss angle and the fraction of edge-sharing versus corner-sharing polyhedra in the medium-range order, as reported in [38] for ZrO$_2$:Ta$_2$O$_5$. SiO$_2$ also has a prevalence of corner sharing, and is the amorphous material that exhibits the lowest known room-temperature loss angle in the acoustic frequency range [22,39,40]. Additionally, the mechanical loss angle of GeO$_2$ at low temperatures [41] ($\lesssim 100$ K) exhibits a peak similar to the one found in SiO$_2$ [42,43]. In recent experiments on GeO$_2$ [44], we confirmed that the atomic packing can be altered to improve medium-range order by annealing and high temperature deposition. Similar correlations were found for different oxides by other groups [45–49].

From the optical perspective, however, GeO$_2$ has a refractive index $n = 1.60$ at 1064 nm that makes it unsuitable for use in a high reflector design when combined with SiO$_2$, as 138 layers would be needed to achieve the required high reflectivity for the test-mass mirrors. The increase in the total thickness of a GeO$_2$/SiO$_2$ reflector would balance out the reduced mechanical loss, with no net improvement in the coating Brownian noise. To increase the refractive index at the laser wavelength of 1064 nm, GeO$_2$ was codeposited with TiO$_2$ with different cation concentrations.

Thin films of TiO$_2$:GeO$_2$ with Ti cation concentration of 0%, 27%, and 44% were deposited by ion beam sputtering using a biased target deposition system [50], that allowed convenient tuning of the mixture composition by adjusting the length of the pulses biasing the metallic Ti and Ge targets.

The cation concentration, oxygen stoichiometry, and atomic areal density of the films were determined by Rutherford backscattering spectrometry (RBS) [51]. The thickness and refractive index were obtained from spectroscopic ellipsometry. The mass density was computed from the RBS and ellipsometry measurements. The absorption loss at the wavelength of 1064 nm was assessed from photothermal common-path interferometry [52]. The thin

films were annealed in air, as annealing has been shown to reduce absorption loss and room-temperature mechanical loss angle in amorphous oxides [53,54]. Grazing incidence x-ray diffraction shows all mixture films are amorphous upon annealing at 600 °C for 10 and 108 hours, and show signs of crystallization when annealed at higher temperatures. The pure GeO$_2$ film remained amorphous up to 550 °C.

For the Ti cation concentration of 44%, the refractive index at 1064 nm is $n_{\text{TiO}_2:\text{GeO}_2} = 1.88$. The absorption loss normalized to a quarter-wavelength (QWL) thick single layer (141 nm) is 2.3 ± 0.1 pp m after annealing at 600 °C. The absorption loss of pure GeO$_2$ after annealing at 500 °C is below 1 ppm at $\lambda = 1064$ nm, showing the potential for improved absorption in the mixture. The deposition parameters are being optimized to achieve even lower optical absorption in TiO$_2$:GeO$_2$, to meet the Advanced LIGO+ requirements of less than 1 ppm [27] for a full mirror coating. More details on the structural and optical characterizations are available in the Supplemental Material [16].

The thin films were also deposited with the same procedure on 75-mm-diameter, 1-mm-thick silica disks, to measure the material's elastic properties. The disk acts as a resonator: about 20 modes between 1 kHz and 30 kHz can be measured in a gentle nodal suspension [55,56] to obtain their precise frequency and decay time. After the thin film is deposited on the substrate, the resonant frequencies are shifted by amounts depending on the film properties, allowing an estimation of the Young's modulus and Poisson ratio [22,57]. The decay times of the modes of the coated substrates are significantly shorter than for the bare substrate, due to the elastic energy dissipation in the film. Using the measured elastic properties of the film material, one can compute the fraction of elastic energy in the film for each resonant mode and use it to extract the loss angle ϕ of the thin-film material [58].

For a homogeneous amorphous material, the relation between stress and strain in the elastic regime can be described in terms of two elastic moduli, for example bulk K and shear μ moduli [59]. Similarly, the internal energy dissipation in the material should be described in terms of two loss angles $\phi_K = \text{Im}(K)/\text{Re}(K)$ and $\phi_\mu = \text{Im}(\mu)/\text{Re}(\mu)$. There is no physical reason to assume the two loss angles to be equal, and we shall show in the following that they are indeed significantly different for TiO$_2$:GeO$_2$. The layered structure of the stack implies that a description in terms of an equivalent isotropic material is not accurate, since the bulk and shear energy distribution in the layers is different in the case of the ring-down measurements and in the Brownian noise case. While the expression in Eq. (1) assumes equal loss angles, a more precise expression, including the distinction between bulk and shear properties for all layers, is described in the Supplemental Material [16], and is needed to correctly account for the multilayer structure and the different materials.
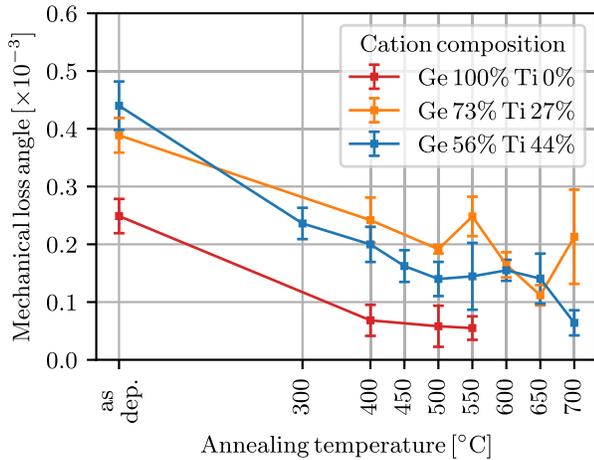
FIG. 1.   Measured loss angle of $TiO_2:GeO_2$, as deposited and after 10-hour-long annealing in air, at increasing temperatures. Different color lines correspond to the cation composition listed in the legend. Only one sample for each concentration is shown here for simplicity. Other samples showed equal values within the error bars.

FIG. 2.   Effect of the annealing duration on the measured loss angle for the 44% $TiO_2:GeO_2$ film.

However, in the initial exploration of the effect of composition and annealing schedule, we relied on the commonly used description with frequency independent equal bulk and shear loss angles [22,60,61]. The more detailed analysis of the best candidate material, described later, supports the use of this simplification for survey purposes, since our measurements are more sensitive to the shear than the bulk loss angle, and the former is found to be almost frequency independent. With this approach, Fig. 1 shows the measured loss angle for pure GeO_2 and the two concentrations of TiO_2 and GeO_2 studied in detail here. The most promising results are from a mixture of 44% TiO_2 and 56% GeO_2. The mechanical loss of amorphous oxides typically decreases with increasing annealing temperature and time. We observed rapid crystallization at 700 °C, and therefore explored the effect of annealing duration on the loss angle. We tested heat treatments of 1, 10, 20, 108, and 216 hours in total, for temperatures of 500, 550, and 600 °C. Figure 2 shows the effect of annealing time on the loss angle of the 44% $TiO_2:GeO_2$ mixture. It was found that extended annealing at lower temperatures produces little improvement. Instead, after annealing at 600 °C for 108 hours, the loss angle is reduced to $(0.96 \pm 0.18) \times 10^{-4}$, and the film is still amorphous. Among those tested in our work, this $TiO_2:GeO_2$ mixture is the most promising high-index material for low Brownian noise Advanced LIGO+ mirrors, though further characterization of mixtures with other Ti/Ge ratios in this range is planned to find the optimum.

As a first step toward the production of a full high-reflectivity coating, and to better characterize this new material, we deposited single layers of SiO_2 and $TiO_2:GeO_2$, as well as a stack of 5 QWL layers of $TiO_2:GeO_2$ alternated with 5 layers of SiO_2, and 20 layers
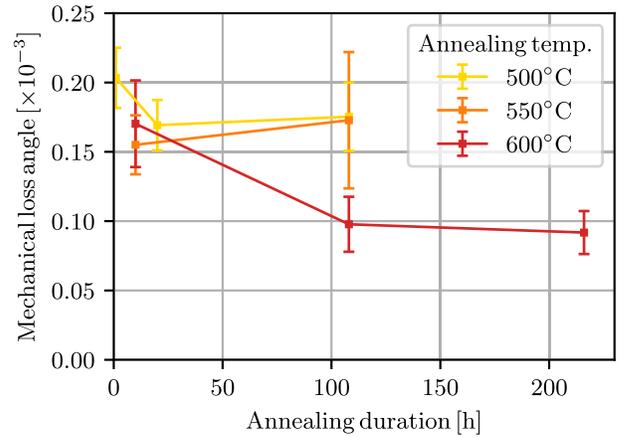
of $TiO_2:GeO_2$ alternated with 20 layers of SiO_2. The depositions were performed using a commercial Spector Ion Beam Sputtering system that can produce films with better optical quality [30] than the biased target system used for the initial parameter exploration. At the laser wavelength of 1064 nm, the transmission of the 40-layer structure was 190 ppm and the optical absorption was measured to be 3.1 ppm after annealing. We also measured the Young's modulus and loss angle of the stacks. However, since the multilayer structure is not isotropic, a description in terms of Y and ν is only approximate. Nevertheless, the two stacks were found to have the same Young's modulus, 78.0 ± 1.3 GPa, and the same loss angle, $(5.5 \pm 0.7) \times 10^{-5}$ after annealing at 600 °C for 108 h. This is an indication that there is no evidence of any systematic error in the measurements due to the thickness of the coatings. At an approximation level consistent with assuming equal bulk and shear loss angles, one can compute the expected value for the stack by averaging the single material values as $\bar{\phi} = \langle Y\phi \rangle / \langle Y \rangle = (6.4 \pm 1.7) \times 10^{-5}$. Therefore there is no indication of excess loss due to interfaces [62].

A correct description of the Brownian noise in a multilayer stack must take into account the bulk and shear moduli and loss angles of the individual materials. The resonant modes of the coated disk store different fractions of bulk and shear energy in the film, and therefore it is possible to extract the bulk and shear loss angles from the measurements [57,63]. We model a single isotropic layer with known thickness and density as measured by ellipsometry and RBS, and with Young's modulus, Poisson ratio, and bulk and shear loss angles as free parameters. For each sample, the measurement data set consists of the frequency shifts due to the coating, and the reduction in the decay time, due to the energy dissipation in the coating, for each of the measurable modes. We used a Markov chain Monte Carlo Bayesian analysis [57,64,65] to find the probability distribution of the model parameters given
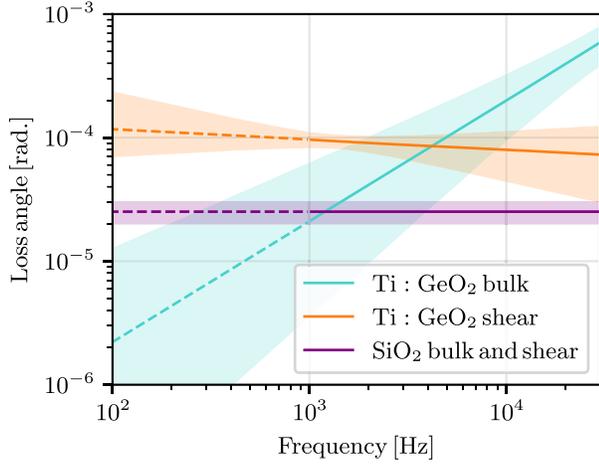
FIG. 3. Estimated bulk and shear loss angles as a function of frequency. The solid lines indicate the range of frequencies where the loss angles were measured, while the dashed lines are extrapolations to the lower frequency range. The shaded regions show the 90% confidence intervals of the estimates.

the data. We considered either different bulk and shear loss angles or equal loss angles, and three possible frequency dependencies, constant, linear, or power law, for a total of six different loss models. The Bayesian analysis allows us to compute the relative likelihood of each model given the data. The best model for the $TiO_2:GeO_2$ film is a power law with different bulk and shear loss angles, while for the SiO_2 film it is a constant single loss angle, as shown in Fig. 3. It is worth noting that the bulk loss angle for the $TiO_2:GeO_2$ film shows a rather steep frequency dependence. The second most likely model for this material is the one with a linear frequency dependence. The bulk loss angle does not show a frequency dependency as steep as in the power law case, but it is still predicted to be significantly smaller than the shear loss angle at low frequency. The measured value of the loss angle for SiO_2 is compatible with values reported in the literature [22]. Table I summarizes all the measured material properties. More details on the analysis and the results are in the Supplemental Material [16].

The transmission requirements for the Advanced LIGO+ test masses are similar to those for Advanced LIGO: the input mirror test masses (ITM) should have a transmission of 1.4% and the end test masses (ETM) of 5 ppm [3]. Given the measured refractive indexes, the ITM stack is composed of 11 layers of 106 nm of $TiO_2:GeO_2$ alternated with 11 layers of 228 nm of SiO_2, while the ETM stack is composed of 26 layers of 123 nm of $TiO_2:GeO_2$ and 26 layers of 207 nm of SiO_2. Both structures are capped with a half-wavelength-thick SiO_2 layer.

The Brownian noise for such mirrors can be computed using the effective medium approach described in the Supplemental Material [16], which has been checked to provide results within a few percentages of other published

TABLE I. Measured parameters for $TiO_2:GeO_2$ and SiO_2, after annealing at 600 °C for 108 hours. The loss angle model for $TiO_2:GeO_2$ is $\phi(f) = a \times (f/10 \text{ kHz})^m$. Uncertainties describe the 90% confidence intervals.

SiO_2 property	Value
Refractive index at 1064 nm	1.45 ± 0.01
Young's modulus	73.2 ± 0.6 GPa
Poisson ratio	0.11 ± 0.07
Loss angle	$\phi_K = \phi_\mu = (2.6^{+0.5}_{-0.6}) \times 10^{-5}$

$TiO_2:GeO_2$ property	Value
Cation concentration $Ti/(Ti + Ge)$	$44.6 \pm 0.3\%$
Refractive index at 1064 nm	1.88 ± 0.01
Optical absorption for a QWL	2.3 ± 0.1 ppm
Density	3690 ± 100 kg/m^3
Young's modulus	91.5 ± 1.8 GPa
Poisson ratio	0.25 ± 0.07
Bulk loss angle	$a_K = (22.0^{+10.6}_{-12.5}) \times 10^{-5}$
	$m_K = 1.04^{+0.40}_{-0.36}$
Shear loss angle	$a_\mu = (8.4^{+2.9}_{-4.0}) \times 10^{-5}$
	$m_\mu = -0.06^{+0.15}_{-0.30}$

formulas [14,66]. The results are shown in Fig. 4. The noise is compliant with the design requirement for Advanced LIGO+, reaching $(5.8^{+1.0}_{-0.7}) \times 10^{-21}$ m/$\sqrt{\text{Hz}}$ at 100 Hz. It is worth noting that this result does not depend strongly on the steep frequency dependency predicted for the bulk loss angle of $TiO_2:GeO_2$. If we use the second most probable model, with a less steep frequency dependency, we obtain
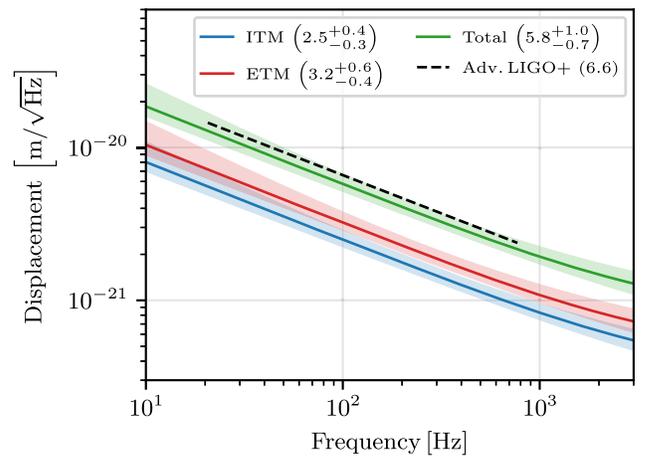
FIG. 4. Estimated Brownian noise for the Advanced LIGO+ interferometer. The red and blue traces show the contribution of a single ITM and ETM, while the green trace shows the total for all four test masses. The numbers in the legend give the Brownian noise level at 100 Hz, in units of 10^{-21} m/$\sqrt{\text{Hz}}$. The shaded regions correspond to the 90% confidence intervals of the estimates. The dashed black line shows the design target for Advanced LIGO+.

$(6.2^{+1.5}_{-0.8}) \times 10^{-21}$ m/$\sqrt{\text{Hz}}$ at 100 Hz, still compatible with the Advanced LIGO+ design requirement. Preparation of samples on disks with lower resonant frequencies to better constrain these estimates is under way.

In summary, we demonstrated that a mixture of 44% TiO_2 and 56% GeO_2 offers excellent optical quality and low mechanical loss angle, making it a promising material to be used as a high-index layer in the test mass coatings of the Advanced LIGO+ interferometric GW detectors. We analyzed the internal energy dissipation of this novel material in terms of bulk and shear loss angles, and used the results to design multilayer high-reflectivity stacks for the Advanced LIGO+ mirrors. The Brownian noise achievable with $TiO_2 : GeO_2 / SiO_2$ based mirrors reaches a level compliant with the Advanced LIGO+ design requirements.

Studies are ongoing to further improve mechanical and optical absorption losses by changing deposition parameters and the mixture and annealing schedule, and to characterize the scattering properties of the multilayer stacks. We are also planning to directly measure the Brownian noise of optimized high reflection mirrors designed for Advanced LIGO+ [24], to confirm the noise prediction.

---

[*]vajente@caltech.edu

[1] B. P. Abbott *et al.* (LIGO Scientific and Virgo Collaborations), Observation of Gravitational Waves from a Binary Black Hole Merger, Phys. Rev. Lett. **116**, 061102 (2016).

[2] B. P. Abbott *et al.* (LIGO Scientific and Virgo Collaborations), GWTC-1: A Gravitational-Wave Transient Catalog of Compact Binary Mergers Observed by LIGO and Virgo during the First and Second Observing Runs, Phys. Rev. X **9**, 031040 (2019).

[3] J. Aasi *et al.*, Advanced LIGO, Classical Quantum Gravity **32**, 074001 (2015).

[4] F. Acernese *et al.*, Advanced Virgo: A second-generation interferometric gravitational wave detector, Classical Quantum Gravity **32**, 024001 (2015).

[5] T. Akutsu *et al.*, KAGRA: 2.5 generation interferometric gravitational wave detector, Nat. Astron. **3**, 35 (2019).

[6] G. Vajente, E. K. Gustafson, and D. H. Reitze, Precision interferometry for gravitational wave detection: Current status and future trends, in *Advances In Atomic, Molecular,*

and Optical Physics (Academic Press, New York, 2019), Vol. 68, ch. 3, pp. 75–148, https://doi.org/10.1016/bs.aamop.2019.04.002.

[7] J. Steinlechner, Development of mirror coatings for gravitational-wave detectors, Phil. Trans. R. Soc. A **376**, 20170282 (2018).

[8] D. V. Martynov *et al.*, Sensitivity of the Advanced LIGO detectors at the beginning of gravitational wave astronomy, Phys. Rev. D **93**, 112004 (2016).

[9] A. Buikema *et al.*, Sensitivity and performance of the Advanced LIGO detectors in the third observing run, Phys. Rev. D **102**, 062003 (2020).

[10] Alessandra Buonanno and Yanbei Chen, Quantum noise in second generation, signal-recycled laser interferometric gravitational-wave detectors, Phys. Rev. D **64**, 042006 (2001).

[11] V. B. Braginsky and S. P. Vyatchanin, Thermodynamical fluctuations in optical mirror coatings, Phys. Lett. A **312**, 244 (2003).

[12] Yu. Levin, Internal thermal noise in the LIGO test masses: A direct approach, Phys. Rev. D **57**, 659 (1998).

[13] H. B. Callen and R. F. Greene, On a theorem of irreversible thermodynamics, Phys. Rev. **86**, 702 (1952).

[14] T. Hong, H. Yang, E. K. Gustafson, R. X. Adhikari, and Y. Chen, Brownian thermal noise in multilayer coated mirrors, Phys. Rev. D **87**, 082001 (2013).

[15] M. M. Fejer, Effective medium description of multilayer coatings, LIGO Document, Report No. T2100186, 2021, https://dcc.ligo.org/LIGO-T2100186/public.

[16] See Supplemental Material at http://link.aps.org/supplemental/10.1103/PhysRevLett.127.071101 for more details on the film deposition and characterization, and on modeling and data analysis, which includes Refs. [17–20].

[17] K. Thamaphat, P. Limsuwan, and B. Ngotawornchai, Phase characterization of TiO_2 powder by XRD and TEM, Agric. Nat. Resour. **42**, 357 (2008), https://li01.tci-thaijo.org/index.php/anres/article/view/244620.

[18] M. Mayer, SIMNRA, a simulation program for the analysis of NRA, RBS and ERDA, AIP Conf. Proc. **475**, 541 (1999).

[19] D. R. M. Crooks, P. Sneddon, G. Cagnoli, J. Hough, S. Rowan, M. M. Fejer, E. Gustafson, R. Route, N. Nakagawa, D. Coyne, G. M. Harry, and A. M. Gretarsson, Excess mechanical loss associated with dielectric mirror coatings on test masses in interferometric gravitational wave detectors, Classical Quantum Gravity **19**, 4229 (2002).

[20] COMSOL multiphysics, https://www.comsol.com.

[21] G. E. Backus, Long-wave elastic anisotropy produced by horizontal layering, J. Geophys. Res. **67**, 4427 (1962).

[22] M. Granata, A. Amato, L. Balzarini, M. Canepa, J. Degallaix, D. Forest, V. Dolique, L. Mereni, C. Michel, L. Pinard, B. Sassolas, J. Teillon, and G. Cagnoli, Amorphous optical coatings of present gravitational-wave interferometers, Classical Quantum Gravity **37**, 095004 (2020).

[23] A. Amato, S. Terreni, V. Dolique, D. Forest, G. Gemme, M. Granata, L. Mereni, C. Michel, L. Pinard, B. Sassolas, J. Teillon, G. Cagnoli, and M. Canepa, Optical properties of high-quality oxide coating materials used in gravitational-wave advanced detectors, J. Phys. **2**, 035004 (2019).

[24] S. Gras and M. Evans, Direct measurement of coating thermal noise in optical resonators, Phys. Rev. D **98,** 122001 (2018).

[25] A. Amato *et al.*, Optical and mechanical properties of ion-beam-sputtered Nb_2O_5 and TiO_2-Nb_2O_5 thin films for gravitational-wave interferometers and an improved measurement of coating thermal noise in Advanced LIGO, Phys. Rev. D **103,** 072001 (2021).

[26] J. Miller, L. Barsotti, S. Vitale, P. Fritschel, M. Evans, and D. Sigg, Prospects for doubling the range of Advanced LIGO, Phys. Rev. D **91,** 062005 (2015).

[27] The LIGO Scientific Collaboration, Instrument Science White Paper 2020, LIGO document, Report No. T2000407, 2020, https://dcc.ligo.org/LIGO-T2000407/public.

[28] X. Liu, D. R. Queen, T. H. Metcalf, J. E. Karel, and F. Hellman, Hydrogen-Free Amorphous Silicon with No Tunneling States, Phys. Rev. Lett. **113,** 025503 (2014).

[29] G. Vajente *et al.*, Effect of elevated substrate temperature deposition on the mechanical losses in tantala thin film coatings, Classical Quantum Gravity **35,** 075001 (2018).

[30] L. Yang, E. Randel, G. Vajente, A. Ananyeva, E. Gustafson, A. Markosyan, R. Bassiri, M. M. Fejer, and C. S. Menoni, Investigation of effects of assisted ion bombardment on mechanical loss of sputtered tantala thin films for gravitational wave interferometers, Phys. Rev. D **100,** 122004 (2019).

[31] L. Yang, E. Randel, G. Vajente, A. Ananyeva, E. Gustafson, A. Markosyan, R. Bassiri, M. Fejer, and C. Menoni, Modifications of ion beam sputtered tantala thin films by secondary argon and oxygen bombardment, Appl. Opt. **59,** A150 (2020).

[32] L. Yang, M. Fazio, G. Vajente, A. Ananyeva, G. Billingsley, A. Markosyan, R. Bassiri, M. M. Fejer, and C. S. Menoni, Structural evolution that affects the room-temperature internal friction of binary oxide nanolaminates: Implications for ultrastable optical cavities, ACS Appl. Nano Mater. **3,** 12308 (2020).

[33] M. A. Fazio, G. Vajente, A. Ananyeva, A. Markosyan, R. Bassiri, M. M. Fejer, and C. S. Menoni, Structure and morphology of low mechanical loss TiO_2-doped Ta_2O_5, Opt. Mater. Express **10,** 1687 (2020).

[34] R. Flaminio, J. Franc, C. Michel, N. Morgado, L. Pinard, and B. Sassolas, A study of coating mechanical and optical losses in view of reducing mirror thermal noise in gravitational wave detectors, Classical Quantum Gravity **27,** 084030 (2010).

[35] M. Abernathy *et al.*, Exploration of co-sputtered Ta_2O_5-ZrO_2 thin films for gravitational-wave detectors, arXiv:2103.14140 [Classical Quantum Gravity (to be published)].

[36] A. Amato, G. Cagnoli, M. Canepa, E. Coillet, J. Degallaix, V. Dolique, D. Forest, M. Granata, V. Martinez, C. Michel, L. Pinard, B. Sassolas, and J. Teillon, High-reflection coatings for gravitational-wave detectors:State of the art and future developments, J. Phys. Conf. Ser. **957,** 012006 (2018).

[37] M. Granata, A. Amato, G. Cagnoli, M. Coulon, J. Degallaix, D. Forest, L. Mereni, C. Michel, L. Pinard, B. Sassolas, and J. Teillon, Progress in the measurement and reduction of thermal noise in optical coatings for gravitational-wave detectors, Appl. Opt. **59,** A229 (2020).

[38] K. Prasai *et al.*, High Precision Detection of Change in Intermediate Range Order of Amorphous Zirconia-Doped Tantala Thin Films Due to Annealing, Phys. Rev. Lett. **123,** 045501 (2019).

[39] S. D. Penn, A. Ageev, D. Busby, G. M. Harry, A. M. Gretarsson, K. Numata, and P. Willems, Frequency and surface dependence of the mechanical loss in fused silica, Phys. Lett. A **352,** 3 (2006).

[40] A. Ageev, B. Cabrera Palmer, A. De Felice, S. D. Penn, and P. R. Saulson, Very high quality factor measured in annealed fused silica, Classical Quantum Gravity **21,** 3887 (2004).

[41] S. Rau, C. Enss, S. Hunklinger, P. Neu, and A. Würger, Acoustic properties of oxide glasses at low temperatures, Phys. Rev. B **52,** 7179 (1995).

[42] K. A. Topp and D. G. Cahill, Elastic properties of several amorphous solids and disordered crystals below 100 K, Z. Phys. B **101,** 235 (1996).

[43] I. W. Martin, R. Nawrodt, K. Craig, C. Schwarz, R. Bassiri, G. Harry, J. Hough, S. Penn, S. Reid, R. Robie, and S. Rowan, Low temperature mechanical dissipation of an ion-beam sputtered silica film, Classical Quantum Gravity **31,** 035019 (2014).

[44] L. Yang, G. Vajente, M. Fazio, A. Ananyeva, G. Billingsley, A. Markosyan, R. Bassiri, K. Prasai, M. M. Fejer, and C. S. Menoni, Enhanced Medium Range Order in Vapor Deposited Germania Glasses at Elevated Temperatures, arXiv:2102.08526.

[45] W. Jin, R. K. Kalia, P. Vashishta, and J. P. Rino, Structural transformation in densified silica glass: A molecular-dynamics study, Phys. Rev. B **50,** 118 (1994).

[46] R. Hamdan, J. P. Trinastic, and H. P. Cheng, Molecular dynamics study of the mechanical loss in amorphous pure and doped silica, J. Chem. Phys. **141,** 054501 (2014).

[47] M. Granata, E. Coillet, V. Martinez, V. Dolique, A. Amato, M. Canepa, J. Margueritat, C. Martinet, A. Mermet, C. Michel, L. Pinard, B. Sassolas, and G. Cagnoli, Correlated evolution of structure and mechanical loss of a sputtered silica film, Phys. Rev. Mater. **2,** 053607 (2018).

[48] A. Amato, S. Terreni, M. Granata, C. Michel, B. Sassolas, L. Pinard, M. Canepa, and G. Cagnoli, Observation of a correlation between internal friction and Urbach energy in amorphous oxides thin films, Sci. Rep. **10,** 1670 (2020).

[49] A. Amato, S. Terreni, M. Granata, C. Michel, L. Pinard, G. Gemme, M. Canepa, and G. Cagnoli, Effect of heating treatment and mixture on optical properties of coating materials used in gravitational-wave detectors, J. Vac. Sci. Technol. B **37,** 062913 (2019).

[50] V. V. Zhurin, H. R. Kaufman, J. R. Kahn, and T. L. Hylton, Biased target deposition, J. Vac. Sci. Technol. A **18,** 37 (2000).

[51] W.-K. Chu, *Backscattering Spectrometry*, 1st ed. (Academic Press, New York, 1978).

[52] A. Alexandrovski, M. Fejer, A. Markosian, and R. Route, Photothermal common-path interferometry (PCI): New developments, in *Solid State Lasers XVIII: Technology and Devices* (International Society for Optics and

Photonics, 2009), Vol. 7193, p. 71930D, https://spie.org/Publications/Proceedings/Paper/10.1117/12.814813?SSO=1.

[53] R. P. Netterfield, M. Gross, F. N. Baynes, K. L. Green, G. M. Harry, H. Armandula, S. Rowan, J. Hough, D. R. M. Crooks, M. M. Fejer, R. Route, and S. D. Penn, Low mechanical loss coatings for LIGO optics: Progress report, in *Advances in Thin-Film Coatings for Optical Applications II*, edited by M. L. Fulton and J. D. T. Kruschwitz (International Society for Optics and Photonics, SPIE, 2005), Vol. 5870, pp. 144–152, https://spie.org/Publications/Proceedings/Paper/10.1117/12.618288.

[54] M. Robert Abernathy, X. Liu, and T. H. Metcalf, An overview of research into low internal friction optical coatings by the gravitational wave detection community, Mater. Res. **21** (2018).

[55] E. Cesarini, M. Lorenzini, E. Campagna, F. Martelli, F. Piergiovanni, F. Vetrano, G. Losurdo, and G. Cagnoli, A gentle nodal suspension for measurements of the acoustic attenuation in materials, Rev. Sci. Instrum. **80**, 053904 (2009).

[56] G. Vajente, A. Ananyeva, G. Billingsley, E. Gustafson, A. Heptonstall, E. Sanchez, and C. Torrie, A high throughput instrument to measure mechanical losses in thin film coatings, Rev. Sci. Instrum. **88**, 073901 (2017).

[57] G. Vajente, M. Fazio, L. Yang, A. Gupta, A. Ananyeva, G. Billinsley, and C. S. Menoni, Method for the experimental measurement of bulk and shear loss angles in amorphous thin films, Phys. Rev. D **101**, 042004 (2020).

[58] T. Li, F. A. Aguilar Sandoval, M. Geitner, L. Bellon, G. Cagnoli, J. Degallaix, V. Dolique, R. Flaminio, D. Forest, M. Granata, C. Michel, N. Morgado, and L. Pinard, Measurements of mechanical thermal noise and energy dissipation in optical dielectric coatings, Phys. Rev. D **89**, 092004 (2014).

[59] L. D. Landau, L. P. Pitaevskii, A. M. Kosevich, and E. M. Lifshitz, *Theory of Elasticity*, 3rd ed. (Elsevier, New York, 1986).

[60] G. M. Harry, A. M. Gretarsson, P. R. Saulson, S. E. Kittelberger, S. D. Penn, W. J. Startin, S. Rowan, M. M. Fejer, D. R. M. Crooks, G. Cagnoli, J. Hough, and N. Nakagawa, Thermal noise in interferometric gravitational wave detectors due to dielectric optical coatings, Classical Quantum Gravity **19**, 897 (2002).

[61] I. Martin and S. Reid, Coating thermal noise, in *Optical Coatings and Thermal Noise in Precision Measurement*, edited by G. Harry, T. P. Bodiya, and R. DeSalvo (Cambridge University Press, Cambridge, England, 2012), p. 31–54, https://doi.org/10.1017/CBO9780511762314.006.

[62] M. Granata, E. Saracco, N. Morgado, A. Cajgfinger, G. Cagnoli, J. Degallaix, V. Dolique, D. Forest, J. Franc, C. Michel, L. Pinard, and R. Flaminio, Mechanical loss in state-of-the-art amorphous optical coatings, Phys. Rev. D **93**, 012007 (2016).

[63] M. Abernathy, G. Harry, J. Newport, H. Fair, M. Kinley-Hanlon, S. Hickey, I. Jiffar, A. Gretarsson, S. Penn, R. Bassiri, E. Gustafson, I. Martin, S. Rowan, and J. Hough, Bulk and shear mechanical loss of titania-doped tantala, Phys. Lett. A **382**, 2282 (2018). Special Issue in memory of Professor V. B. Braginsky.

[64] A. Gelman, J. B. Carlin, H. S. Stern, D. B. Dunson, A. Vehtari, and D. B. Rubin, *Bayesian Data Analysis*, 3rd ed. (Chapman and Hall, London, 2013).

[65] D. Foreman-Mackey, D. W. Hogg, D. Lang, and J. Goodman, emcee: The MCMC hammer, Publ. Astron. Soc. Pac. **125**, 306 (2013).

[66] W. Yam, S. Gras, and M. Evans, Multimaterial coatings with reduced thermal noise, Phys. Rev. D **91**, 042002 (2015).